



Development of Nanobody-Based Flow-through Dot ELISA and Lateral-flow Immunoassay for Rapid Detection of 3- Phenoxybenzoic acid

Journal:	<i>Analytical Methods</i>
Manuscript ID	AY-ART-01-2021-000129.R2
Article Type:	Paper
Date Submitted by the Author:	03-Mar-2021
Complete List of Authors:	Zhang, Can; Jiangsu University, School of Food & Biological Engineering Wu, Xiaoxiao; Jiangsu University Li, Dongyang; University of California, Davis, Department of Entomology and UCD Comprehensive Cancer Center Hu, Jinnuo; Jiangsu University Wan, Debin; University of California Davis Zhang, Zhen; School of the Environment, Jiangsu University, Hammock, Bruce; University of California,

1
2
3
4 1 **Development of Nanobody-Based Flow-through Dot ELISA and Lateral-flow**
5
6 2 **Immunoassay for Rapid Detection of 3-Phenoxybenzoic Acid**

7 3 Can Zhang^{a,b*}, Xiaoxiao Wu^a, Dongyang Li^b, Jinnuo Hu^a, Debin Wan^b, Zhen Zhang^c, Bruce D
8
9 4 Hammock^b
10

11 5
12
13 6 *^a School of Food & Biological Engineering, Jiangsu University, Zhenjiang 212013, China*

14
15 7 *^b Department of Entomology and Nematology and UCD Comprehensive Cancer Center, University of*
16
17 8 *California, Davis, California 95616*

18
19 9 *^c School of the Environment and Safety Engineering, Jiangsu University, Zhenjiang, 212013, China*
20

21 10
22
23 11 E-mail address: zhangcan@mail.ujs.edu.cn
24

25 12
26
27 13 Tel.: +86 0511 88780201
28

1
2
3
4 30 **Abstract**
5

6 31 As a major metabolite of pyrethroids pesticide, 3-phenoxybenzoic acid (3-PBA) can
7
8 32 be an indicator of health risk and human exposure assessment. Based on nanobodies
9
10 33 (Nbs), we have developed a rapid flow-through dot enzyme linked immunosorbent
11
12 34 assay (dot ELISA) and gold nanoparticles (GNPs) lateral-flow immunoassay for
13
14 35 detecting 3-PBA. The limit of detection (LOD) values for detecting 3-PBA by
15
16 36 flow-through dot ELISA and GNPs lateral-flow immunoassay were 0.01 ng mL⁻¹ and
17
18 37 0.1 ng mL⁻¹, respectively. The samples (urine and lake water) with and without 3-PBA
19
20 38 were detected by both nanobody-based flow-through dot ELISA and GNPs
21
22 39 lateral-flow immunoassay, as well as liquid chromatography-mass spectrometry
23
24 40 (LC-MS) for validation. The results between immunoassays showed good consistency.
25
26 41 It demonstrated that the two developed nanobody-based immunoassays are suitable
27
28 42 for rapid detection of 3-PBA.
29

30 43

31 44 **Keywords:** 3-phenoxybenzoic acid, nanobody, gold nanoparticles, flow-through,
32
33 45 lateral-flow, immunoassay
34
35
36
37
38
39
40
41
42
43
44
45
46
47
48
49
50
51
52
53
54
55
56
57
58
59
60

1. Introduction

3-PBA is a common metabolite of a class of pyrethroid pesticides, such as fenpropathrin, cyhalothrin, flucythrinate, permethrin, which can be used as a criterion of exposure assessment in the environment.¹⁻³ Compared with the pyrethroid compounds, it is regarded relatively non-toxic. However, people may unconsciously ingest food contaminated by pyrethroids.^{4,5} Besides, people may also get exposure to 3-PBA through environmental media such as water. Research showed that 3-PBA mainly exists in human urine and blood, and the effect on estrogen of 3-PBA can cause the organism endocrine metabolism disorder.⁶ Therefore, people pay more attention to monitoring and assessing of 3-PBA.

Some methods have been established to detect 3-PBA, including instrumental analysis methods (e.g. high-performance liquid chromatography,^{7,8} supercritical fluid chromatography,⁹ gas chromatography-mass spectrometry¹⁰⁻¹³) and immunoassays (e.g. enzyme immunoassay,¹⁴⁻¹⁷ electrochemical immunoassay,^{18,19} fluorescence immunoassay^{20,21}). Instrumental methods are of high sensitivity and easy automation. However, the cost is high and the sample's clean-up is complex and time-consuming. Traditional ELISA, especially membrane-based immunoassay, is suitable for high throughput screening because of its sensitivity and visual evaluation.²² For the establishment of sensitive membrane-based immunoassay, the selection of antibodies plays a key role.

In the past, most of the antibodies (Abs) used for detecting 3-PBA were monoclonal antibodies (mAbs) and polyclonal antibodies (pAbs).²³⁻²⁵ Liu et al established membrane-based immunoassay which used colloidal gold labeled mAbs for detecting 3-PBA in river water and the LOD value was $1 \mu\text{g mL}^{-1}$.²⁶ As the genetic engineering techniques developed, various small size Abs have been found. A new subclass of Abs in members of the camelid family was discovered and called as heavy-chain Abs.²⁷ Recombinant expression of the heavy chain variable domains yield are known as nanobodies (Nbs).²⁸ Compared with traditional Abs (pAbs and mAbs), Nbs have many

1
2
3
4 74 advantages, including thermostability, accessibility and strong specificity.^{29,30} With
5
6 75 the extensive development of Nbs, Nbs were gradually applied in the field of
7
8 76 detection, such as pathogen diagnosis and pollutants detection.^{31,32} Kim¹⁴ et al first
9
10 77 isolated VHH establishing VELISA for detecting 3-PBA, and half-maximal inhibitory
11
12 78 concentration (IC₅₀) could reach to 1.4 ng mL⁻¹ after the fifth round of panning. To
13
14 79 improve sensitivity of 3-PBA detection, Huo¹⁷ et al used nanobody-alkaline
15
16 80 phosphatase fusion protein to develop the direct competitive fluorescence enzyme
17
18 81 immunoassay (dc-FEIA), which achieved LOD as of 0.011 ng mL⁻¹. Sun et al
19
20 82 established a nanobody-based competitive dot ELISA for visual screening of
21
22 83 ochratoxin A in cereals, and the cut-off level of this visualization assessment was 5 µg
23
24 84 kg⁻¹.³³

25
26 85 In this research, nanobodies-based flow-through dot enzyme linked immunosorbent
27
28 86 assay (Nbs-based flow-through dot ELISA) and gold nanoparticles labeled
29
30 87 nanobodies lateral-flow immunoassay (GNPs-Nbs lateral-flow immunoassay), which
31
32 88 used nitrocellulose membrane as supporter, were established for sensitive and rapid
33
34 89 detection of 3-PBA. To verify the reliability of the rapid assays, health volunteers'
35
36 90 urine and lake water were selected for analysis and the results were consistent with
37
38 91 that of LC-MS method. Due to the advantages of high sensitivity, rapid detection and
39
40 92 low-cost, these developed membrane-based immunoassays using Nbs can be applied
41
42 93 as effective and convenient screening tools for monitoring 3-PBA residues in
43
44 94 biological matrix or environment matrix.

95 2. Materials and Methods

96 2.1 Chemicals and Reagents

97 3-PBA standard was purchased from Aladdin (Shanghai, China). Bovine serum
98 albumin (BSA) was purchased from Sigma-Aldrich. Chloroauric acid
99 ($\text{HAuCl}_4 \cdot 4\text{H}_2\text{O}$), trisodium citrate, Tween-20 and methanol were obtained from
100 Sinopharm (Shanghai Sinopharm Group Chemical reagent Co., Ltd.). 6*his-tag
101 monoclonal antibody (McAb) (Cat No: 66005-1-1g) and HRP-conjugated 6*his-tag
102 McAb (Cat No: HRP-66005) were purchased from Proteintech Group, Inc.
103 3,3',5,5'-tetramethylbenzidine (TMB) was purchased from Huinuo Biotechnology
104 (Shenzhen, China). The coating antigen (3-PBA-BSA) and Escherichia coli TOP10F'
105 strain used to express anti-3-PBA nanobodies containing plasmid were provided by
106 Hammock Lab.¹⁴ After expression and purification, the concentration of obtained
107 anti-3-PBA Nbs was 0.3 mg mL^{-1} . Other chemicals were of analytical grade. Two
108 types of nitrocellulose (NC) membrane were purchased from Merck Millipore Ltd
109 (Cat No: HATF00010 and HF13502S25).

110 2.2 Nbs-based Flow-through Dot ELISA

111 The pre-treatment of NC membrane for flow-through dot ELISA was prepared with
112 slight modification as the reference described.³³ Briefly, slight marks were made at
113 center areas to located the reaction zone on the membrane and the membrane was
114 immersed into PBS buffer for activation. Five μL coating antigen of 3-PBA-BSA (75
115 $\mu\text{g mL}^{-1}$) was dropped onto reaction zone. After the liquid flowed through, the
116 membrane was blocked by immersing in PBS solution containing 3% non-powered
117 milk (m/v) for 1 h. Finally, the membranes were washed, dried at room temperature,
118 and stored at 4°C until use.

119 Nbs-based flow-through dot ELISA for 3-PBA detection was performed as following
120 procedures: firstly, different concentrations of 3-PBA solution and anti-3-PBA Nbs
121 were pre-mixed, then dropped onto the reaction zone. After the liquid flowed through
122 the membrane completely, the membrane was washed with PBST. Then $5 \mu\text{L}$ of 500-

1
2
3
4 123 fold-diluted secondary antibody (HRP-conjugated 6*his-tag McAb) was added.
5
6 124 Finally, the NC membrane was immersed in TMB substrate solution for coloration.
7
8 125 After 10 min, color of each dot was visually judged by comparing with negative
9
10 126 control (without 3-PBA).

11 127 **2.3 Gold Nanoparticles Labeled Nbs (GNPs-Nbs)**

12
13
14 128 Gold nanoparticles (GNPs) with diameter about 20 nm were prepared according to the
15
16 129 procedure described by Frens.³⁴ Briefly, 100 mL of 0.01% HAuCl₄ solution (in Milli-Q
17
18 130 purified water) was boiling thoroughly. Then 1% trisodium citrate solution was added
19
20 131 under constant stirring. The generated GNPs colloidal was cooled to room
21
22 132 temperature and stored at 4 °C until use.

23
24 133 For protein labeling of GNPs, protein has the best adsorption capacity when the pH
25
26 134 value is closed to its isoelectric point ($\text{pH} \geq \text{pI}$).³⁵ The pH of GNPs was adjusted by
27
28 135 adding different amounts of K₂CO₃. For 1 mL GNPs solution, 0.2 mol L⁻¹ K₂CO₃ of
29
30 136 different volume (5, 10, 15, 20, 25, 30, 50 and 100 μL) were separately added to
31
32 137 adjust pH value. The excess Nbs were added into the GNPs solution containing
33
34 138 different amounts of K₂CO₃ and incubated for 1 h. Then each tube was added 50 μL of
35
36 139 10% NaCl and kept for 30 min before scanning under 400-600 nm. The amount of
37
38 140 K₂CO₃ corresponding to the value at λ_{max} was chosen for regulation of GNPs solution
39
40 141 before coupling with Nbs. The procedure performed three times repeatedly. Once the
41
42 142 optimal pH condition was set, different amounts of 0.3 mg mL⁻¹ Nbs (5, 10, 15, 20, 25
43
44 143 and 30 μL) were also optimized according to the same procedure. GNPs-Nbs were
45
46 144 centrifuged for 30 min at 10000 rpm, the sediment was dissolved with storage buffer
47
48 145 (containing 1% BSA and 0.25% Tween-20).

49 146 **2.4 GNPs-Nbs Lateral-flow Immunoassay**

50
51
52 147 The NC membrane for GNPs-Nbs lateral-flow immunoassay was prepared according
53
54 148 to the reference by Zhang.³⁶ One microliter of 50 $\mu\text{g mL}^{-1}$ 3-PBA-BSA was coated as
55
56 149 test zone and 1 μL of 6*his-tag McAb (20-fold diluted) was coated as control zone.
57
58 150 The mixed solution containing GNPs-Nbs (10-fold diluted) and different
59
60

1
2
3
4 151 concentrations of 3-PBA was dropped onto the beginning site of the membrane until
5
6 152 the liquid migrated across test zone and control zone completely.

7 153 **2.5 Cross-reactivity**

9
10 154 To assess the specificity of the competitive immunoassay, cross-reactivity (CR) of
11
12 155 anti-3-PBA Nbs with structural analogues (3-phenoxybenzaldehyde, 3-phenoxybenzyl
13
14 156 alcohol and 4-(3-hydroxybenoxy) benzoic acid) were also determined by Nbs-based
15
16 157 flow-through dot ELISA and GNPs-Nbs lateral-flow immunoassay.

17 158 **2.6 Matrix Effect and Sample Analysis**

19
20 159 To evaluate matrix effect, a series of concentrations of 3-PBA were prepared in 10%
21
22 160 methanol/PBS (as standard) and negative sample matrix. They were measured using
23
24 161 plate ELISA, flow-through dot ELISA and lateral-flow immunoassay. To facilitate the
25
26 162 quantitative analysis of flow-through dot ELISA and lateral-flow immunoassay, we
27
28 163 also used Adobe Photoshop CC software to analyze the images of standard solution,
29
30 164 and calculated the inhibition ratio by comparing the grayscale difference of the dot's
31
32 165 color to get the standard curve.

33
34 166 We took urine samples from healthy volunteers and lake water from Jiangsu
35
36 167 University with no exposure to pyrethroid insecticides for spiking analysis. Urine
37
38 168 collection was performed following the guidelines and protocols of the Jiangsu
39
40 169 University. They were proved to be non-3-PBA by LC-MS analysis. The urine
41
42 170 samples were centrifuged at 10000 rpm for 10 min, and the supernatant was filtered
43
44 171 by 0.22 μm filter membrane before immunoassays. The lake water was directly
45
46 172 analyzed after filtration. Sample treatment for LC-MS analysis was the same as
47
48 173 described by Huo.¹⁷

49
50
51 174 Negative samples confirmed to be free of 3-PBA by LC-MS were spiked with 3-PBA
52
53 175 at concentrations of 0.1, 1, 10, 50 ng mL^{-1} for recovery analysis. The recovery
54
55 176 analysis was done repeatedly four times. We also used software to quantitatively
56
57 177 analyze the images of the visual results, and validated by LC-MS to get the
58
59 178 correlation. Negative samples were also randomly spiked with 3-PBA and
60

1
2
3
4 179 simultaneously analyzed using Nbs-based flow-through dot ELISA, GNPs-Nbs
5
6 180 lateral-flow immunoassays and LC-MS.

181 **3. Results and Discussion**

182 **3.1 Nbs-based Flow-through Dot ELISA**

183 To get better visual judgement, we first performed the optimization of experimental
184 parameters. The concentration of Nbs and HRP-conjugated 6*his-tag McAb were
185 optimized by checkerboard titration (Figure 1a). The color of dot faded down as the
186 concentration of Nbs decreased from 25 $\mu\text{g mL}^{-1}$ to 3.125 $\mu\text{g mL}^{-1}$. With the dilution
187 of HRP-conjugated 6*his-tag McAb increased, the dot color was getting weak. For
188 flow-through dot ELISA, Nbs at the concentration of 25 $\mu\text{g mL}^{-1}$ and 500-fold diluted
189 HRP-conjugated 6*his-tag McAb were applied for the following analysis. A series of
190 concentrations of 3-PBA were added for competitive immunoassay. In the method, the
191 reaction is competitive combination of coating antigen and free 3-PBA with Nbs.
192 When the concentration of free 3-PBA was too high, Nbs could combine with it
193 completely in the mixture. There was no excess Nbs to combine with the coating
194 antigen on the membrane, so the test zone was colorless. The intensity of dot's color
195 was inversely proportional to the increased concentration of 3-PBA. When the
196 concentration of 3-PBA reached to 0.01 ng mL^{-1} (Figure 1b), the dot color could be
197 still distinguished from negative control (without 3-PBA), which was defined as
198 cutoff value for Nbs-based flow-through dot ELISA.

199 200 **3.2 Optimization of Gold Nanoparticles Labeled Nbs**

201 In the process of labeling, the pH value played a key role. The pH value of GNPs
202 solution was adjusted by adding different amounts of K_2CO_3 . Figure 2a shows the pH
203 effect on labeling, along with the volume of K_2CO_3 increased from 0 to 100 μL , the
204 absorbance of λ_{max} reaches maximum value with the amount of 20 μL K_2CO_3 , and the
205 conjugation between GNPs and Nbs reached the best stable state. With gradually
206 increased amount of Nbs (Figure 2b) at the optimum pH, the maximum absorption
207 peak and its corresponding absorbance almost kept constant and reached the optimal
208

1
2
3
4 208 conjugation state when the amount of Nbs was 15 μL (at the concentration of 0.3 mg
5 209 mL^{-1}). Based on these parameters, for 1 mL GNPs solution, the optimum labeling
6 210 conditions were 20 μL K_2CO_3 (0.2 mol L^{-1}) for pH adjustment and 15 μL Nbs (0.3 mg
7 211 mL^{-1}) for conjugation. The GNPs and GNPs labeled Nbs were characterized by
8 212 wavelength scanning from 400 to 600 nm. After conjugation, λ_{max} of GNPs had a
9 213 redshift from 520 nm to 525 nm, which could preliminarily indicate successful
10 214 conjugation (Figure 3a). The characterizations of GNPs and GNPs-Nbs analyzed by
11 215 the transmission electron microscope (TEM) and particle size analyzer are shown in
12 216 Figure S1. From the images of TEM, both GNPs and GNPs-Nbs are well-dispersed
13 217 without aggregation. The particle size of GNPs-Nbs reached to 30 nm, while the size
14 218 of bare GNPs was about 20 nm (Figure 3b). To further verify the successful
15 219 conjugation, both GNPs and GNPs-Nbs were selected for lateral-flow immunoassay
16 220 (Figure 3c). GNPs did not form red spots on the NC membrane (Figure 3c-A), and
17 221 GNPs-Nbs showed red spots which indicated specific binding between coating
18 222 antigen and GNPs-Nbs (Figure 3c-B) for successful conjugation.
19 223

224 3.3 GNPs-Nbs Based Lateral-flow Immunoassay

225 Figure 4 shows the competitive GNPs-Nbs lateral-flow immunoassay for 3-PBA
226 detection. The Nbs firstly mixed with 3-PBA, and along with the increasing
227 concentration of 3-PBA, the color of test zone gradually faded down. When the
228 concentration of 3-PBA was more than 0.1 ng mL^{-1} , the color of test zone could be
229 easily distinguished from the color of test zone without 3-PBA. Thus, the LOD of
230 GNPs-Nbs lateral-flow immunoassay was determined to be 0.1 ng mL^{-1} .

232 3.4 Cross-reactivity Analyzed by Nbs-based Flow-through Dot ELISA and 233 GNPs-Nbs Lateral-flow Immunoassay

234 Nbs-based flow-through dot ELISA and GNPs-Nbs lateral-flow immunoassay were
235 also applied for the detection of other structural analogues (3-phenoxybenzaldehyde,
236 3-phenoxybenzyl alcohol and 4-(3-hydroxybenoxy) benzoic acid). The specificity and

1
2
3
4 237 validation of the developed assays were studied. As shown in Table 1, the
5
6 238 concentrations of 0.1 ng mL^{-1} and 1 ng mL^{-1} were selected for cross-reactivity
7
8 239 analysis. The analogues of 3-phenoxybenzaldehyde and 4-(3-hydroxybenoxy) benzoic
9
10 240 acid had the cross-reactivity of 75.1% and 13.5% by plate ELISA, and
11
12 241 3-phenoxybeneyl alcohol showed no cross-reactivity with 3-PBA ($<0.1\%$). The results
13
14 242 also indicated that the higher cross-reactivity led to the more similar detection
15
16 243 images by Nbs-based flow-through dot ELISA and GNPs-Nbs lateral-flow
17
18 244 immunoassay.

20 245 **3.5 Sample Analysis**

21
22 246 We studied the influence of negative urine and lake water as matrix on Nbs-based
23
24 247 flow-through dot ELISA, GNPs-Nbs lateral-flow immunoassay and plate ELISA. A
25
26 248 series of concentrations of 3-PBA were separately dissolved in 10% methanol/PBS
27
28 249 and negative samples matrix. The detection results of the three immunoassays were
29
30 250 compared and showed good consistency (Figure S2). For Nbs-based flow-through dot
31
32 251 ELISA and GNPs-Nbs lateral-flow immunoassay, the influence of matrix almost can
33
34 252 be ignored. The images were captured by smartphone and analyzed by software, the
35
36 253 gray scale and standard curve of two methods were shown in Figure S3. The cutoff
37
38 254 levels which defined as the concentration corresponding to 10% inhibition ratio, were
39
40 255 0.01 ng mL^{-1} and 0.1 ng mL^{-1} , respectively. The results were also consistent with that
41
42 256 of visual judgement results.

43
44 257 To evaluate the validation of Nbs-based flow-through dot ELISA and GNPs-Nbs
45
46 258 lateral-flow immunoassay, we spiked 3-PBA in negative urine samples at the
47
48 259 concentrations of 0.1, 1, 10, 50 ng mL^{-1} . Figure 5 shows that the dot color faded down
49
50 260 when the spiked concentration increased. The recoveries by LC-MS ranged from 97%
51
52 261 to 103% (Table 2). The quantitatively analysis of the visual results showed in Table
53
54 262 S1. And correlation curves of flow-through dot ELISA ($R^2=0.982$) and GNPs-Nbs
55
56 263 lateral-flow immunoassay ($R^2=0.973$) between LC-MS showed good consistent
57
58 264 (Figure S4). We also used the data to obtain ROC curves in Supplementary Materials
59
60

1
2
3
4 265 (Figure S5). The results showed that the cut off value of flow-through dot ELISA and
5 266 lateral-flow immunoassay were 0.011 ng mL^{-1} and 0.107 ng mL^{-1} , which was
6
7 267 consistent with visual results. We also randomly spiked 3-PBA on negative samples
8
9 268 and analyzed by Nbs-based flow-through dot ELISA and GNPs-Nbs lateral-flow
10
11 269 immunoassay (Table 3). The visual results by flow-through dot ELISA ($3\text{-PBA} > 0.1$
12
13 270 ng mL^{-1}) showed good consistency with LC-MS. As well, the results by lateral-flow
14
15 271 immunoassay ($3\text{-PBA} > 0.1 \text{ ng mL}^{-1}$) showed good consistency with LC-MS.
16
17 272 Therefore, the developed Nbs-based flow-through dot ELISA and GNPs-Nbs
18
19 273 lateral-flow immunoassay demonstrated to be the practicable biological monitoring
20
21 274 methods for rapid screening of 3-PBA.
22

23 275

24 276 **4. Conclusion**

25
26
27 277 We developed two formats (flow-through and lateral-flow) of rapid and convenient
28
29 278 Nbs-based immunoassays for 3-PBA detection. The results can be evaluated by the
30
31 279 color change of reaction zone which could be directly judged by naked eyes. The
32
33 280 LOD value of GNPs-Nbs based lateral-flow immunoassay for 3-PBA detection was
34
35 281 0.1 ng mL^{-1} , which was 100-fold sensitive than mAbs-based lateral-flow immunoassay
36
37 282 reported by Liu.²⁶ The flow-through dot ELISA was more sensitive, but the process of
38
39 283 GNPs-Nbs lateral-flow immunoassay was more convenient because there was no step
40
41 284 for substrate participation and the detection time is within 10 min. The spiked samples
42
43 285 were tested by Nbs-based flow-through dot ELISA and GNPs-Nbs lateral-flow
44
45 286 immunoassay, which showed consistence with the results of LC-MS. As Nbs have the
46
47 287 advantage for anti-matrix interference, samples can be analyzed without complicated
48
49 288 treatments. Moreover, the membrane-based immunoassays (flow-through and
50
51 289 lateral-flow) perform the operation more quickly than instrumental methods for high
52
53 290 throughput sample analysis. Therefore, Nbs-based flow-through dot ELISA and
54
55 291 GNPs-Nbs lateral-flow immunoassay are suitable for visual evaluation and
56
57 292 qualitatively on-site sensitive detection of 3-PBA in biological matrix and
58
59 293 environmental matrix.
60

1
2
3
4 294 **Ethical Approval**
5

6 295 All applicable procedures for the use of urines were approved by the Ethical
7
8 296 Committee of Jiangsu University and performed following the guidelines and
9
10 297 protocols of Jiangsu University.
11

12 298 **Author Contributions**
13

14 299 Can Zhang: Conceptualization, Methodology, Resources, Writing – Review & Editing,
15
16 300 Supervision.
17

18
19 301 Xiaoxiao Wu: Methodology, Formal Analysis, Investigation, Data Curation,
20
21 302 Writing-Original draft, Visualization.
22

23
24 303 Dongyang Li, Jinnuo Hu & Debin Wan: Writing – Review & Editing.
25

26 304 Zhen Zhang: Resources.
27

28
29 305 Bruce D Hammock: Resources, Funding Acquisition, Supervision.
30

31 306 **Conflicts of interest**
32

33 307 There are no conflicts to declare.
34

35 308 **Acknowledgments**
36

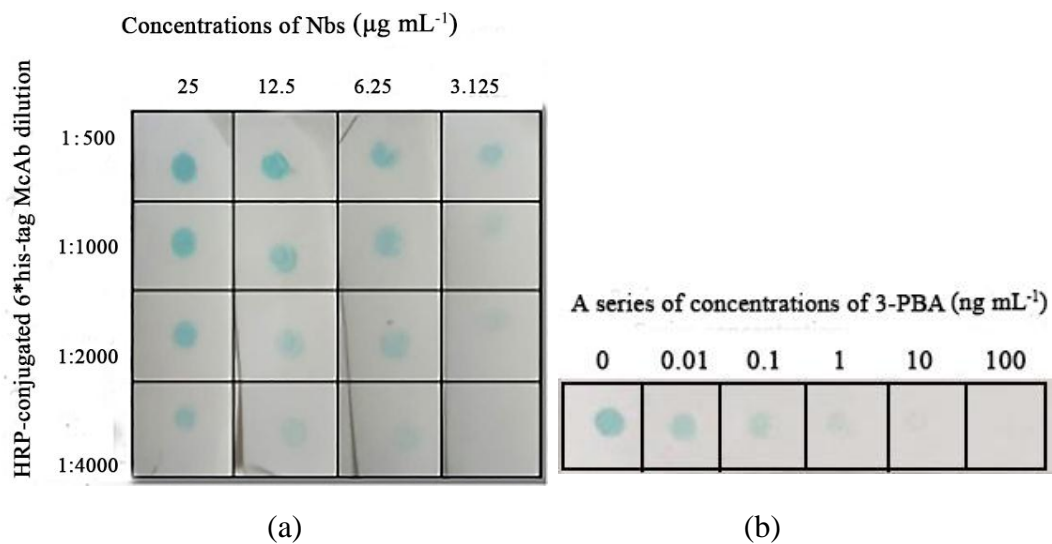
37
38 309 We are very grateful to volunteers for providing samples. We are very grateful to Dr
39
40 310 Wan for LC-MS analysis. This work was financially supported by the National
41
42 311 Institute of Environmental Health Science Superfund Research Program
43
44 312 (P42ES004699). Any opinions, findings, conclusions, or recommendations expressed
45
46 313 in such article are those of the authors alone, and do not necessarily reflect the views
47
48 314 of USAID or NAS.
49
50
51
52
53
54
55
56
57
58
59
60

315 **References**

- 316 1. G. M. Shan, H. Z. Huang, D. W. Stoutamire, S. J. Gee, G. Leng and B. D.
317 Hammock, *Chem. Res. Toxicol.*, 2004, **17**(2), 218-225.
- 318 2. D. L. Sudakin, *Clin. Toxicol.*, 2006, **44**(1), 31-37.
- 319 3. L. Chen, T. F. Zhao, C. P. Pan, J. H. Ross and R. I. Krieger, *J. Agric. Food Chem.*,
320 2012, **60**(36), 9342-9351.
- 321 4. J. R. Richardson, M. M. Taylor, S. L. Shalat, T. S. Guillot, W. M. Caudle, M. M.
322 Hossain, T. A. Mathews, S. R. Jones, D. A. Cory-Slechta and G. W. Miller, *FASEB J.*,
323 2015, **29**(5), 1960-1972.
- 324 5. K. M. Erstfeld, *Chemosphere.*, 1999, **39**(10), 1737-1769.
- 325 6. M. Morgan, P. Jones, J. Sobus and D. B. Boyd, *Int. J. Environ. Res. Public Health.*,
326 2016, **13**(11), 1172.
- 327 7. Y. Ding, C. A. White, S. Muralidhara, J. V. Bruckner and M. G. Bartlett, *J.*
328 *Chromatogr. B: Anal. Technol. Biomed. Life Sci.*, 2004, **810**(2), 221-227.
- 329 8. A. W. Abu-Qare and M. B. Abou-Donia, *J. Anal. Toxicol.*, 2001, **25**(4), 275-279.
- 330 9. M. H. El-Saeid and H. A. Khan, *Int. J. Food Prop.*, 2015, **18**(5), 1119-1127.
- 331 10. M. K. Mudiam, A. Chauhan, R. Jain, Y. K. Dhuriya, P. N. Saxena and V. K.
332 Khanna, *J. Chromatogr. B: Anal. Technol. Biomed. Life Sci.*, 2014, **945-946**, 23-30.
- 333 11. S. Saito, J. Ueyama, T. Kondo, I. Saito, E. Shibata, M. Gotoh, H. Nomura, S.
334 Wakusawa, K. Nakai and M. Kamijima, *J. Exposure Sci. Environ. Epidemiol.*, 2014,
335 **24**(2), 200-207.
- 336 12. I. Bragança, P. C. Lemos, C. Delerue-Matos and V. F. Domingues, *Environ. Sci.*
337 *Pollut. Res.*, 2019, **26**(3), 2987-2997.
- 338 13. M. P. Kavvalakis, M. N. Tzatzarakis, A. K. Alegakis, D. Vynias, A. K. Tsakalof
339 and A. M. Tsatsakis, *Drug Test. Anal.*, 2014, **6** (Suppl 1), 9-16.
- 340 14. H. J. Kim, M. R. McCoy, Z. Majkova, J. E. Dechant, S. J. Gee, S. Tabares-da
341 Rosa, G. G. Gonzalez-Sapienza and B. D. Hammock, *Anal. Chem.*, 2012, **84**(2),
342 1165-1171.
- 343 15. S. Thiphom, T. Prapamontol, S. Chantara, A. Mangklabruks, C. Suphavitai, K. C.

- 1
2
3
4 344 Ahn, S. J. Gee and B. D. Hammock, *J. Environ. Sci. Health, Part B.*, 2014, **49**(1),
5 345 15-22.
6
7 346 16. K. C. Ahn, S. J. Gee, H. J. Kim, P. A. Aronov, H. Vega, R. I. Krieger and B. D.
8 Hammock, *Anal. Bioanal. Chem.*, 2011, **401**(4), 1285-1293.
9 347
10 348 17. J. Q. Huo, Z. F. Li, D. B. Wan, D. Y. Li, M. Qi, B. Barnych, N. Vasylieva, J. L.
11 Zhang and B. D. Hammock, *J. Agric. Food Chem.*, 2018, **66**(43), 11284-11290.
12 349
13 350 18. A. Y. El-Moghazy, J. Q. Huo, N. Amaly, N. Vasylieva, B. D. Hammock and G.
14 Sun, *ACS Appl. Mater. Interfaces.*, 2020, **12**(5), 6159-6168.
15 351
16 352 19. M. Pali, C. R. S. Bever, N. Vasylieva, B. D. Hammock and I. I. Suni,
17 *Electroanalysis.*, 2018, **30**(11), 2653-2659.
18 353
19 354 20. Y. L. Wang, Z. F. Li, B. Barnych, J. Q. Huo, D. Wan, N. Vasylieva, J. L. Xu, P. Li,
20 B. B. Liu, C. Z. Zhang and B. D. Hammock, *J. Agric. Food Chem.*, 2019, **67**(41),
21 355 11536-11541.
22 356
23 357 21. M. Nichkova, D. Dosev, A. E. Davies, S. J. Gee, I. M. Kennedy and B. D.
24 Hammock, *Anal. Lett.*, 2007, **40**(7), 1423-1433.
25 358
26 359 22. C. Y. Zhao, Y. Si, B. F. Pan, A. Y. Taha, T. R. Pan and G. Sun, *Talanta.*, 2020, **217**,
27 360 121054.
28 361
29 362 23. H. J. Kim, K. C. Ahn, A. González-Techera, G. G. González-Sapienza, S. J. Gee
30 and B. D. Hammock, *Anal. Biochem.*, 2009, **386**(1), 45-52.
31 363
32 364 24. H. J. Kim, S. J. Gee, Q. X. Li and B. D. Hammock, *ACS Symp. Ser.*, 2007, **966**,
33 365 171-185.
34 366
35 367 25. Y. Lu, N. Xu, Y. Zhang, B. Liu, Y. Song and S. Wang, *Food Agric. Immunol.*,
36 368 2010, **21**(1), 27-45.
37 369
38 370 26. Y. Liu, A. H. Wu, J. Hu, M. M. Lin, M. T. Wen, X. Zhang, C. X. Xu, X. D. Hu, J.
39 F. Zhong, L. X. Jiao, Y. J. Xie, C. Z. Zhang, X. Y. Yu, Y. Liang and X. J. Liu, *Anal.*
40 *Biochem.*, 2015, **483**, 7-11.
41 371
42 372 27. C. Hamers-Casterman, T. Atarhouch, S. Muyldermans, G. Robinson, C. Hamers, E.
43 B. Songa, N. Bendahman and R. Hamers, *Nature.*, 1993, **363**, 446-448.
44
45
46
47
48
49
50
51
52
53
54
55
56
57
58
59
60

- 1
2
3
4 372 28. D. R. Maass, J. Sepulveda, A. Pernthaner and C. B. Shoemaker, *J. Immunol.*
5
6 373 *Methods.*, 2008, **324**(1-2), 13-25.
7
8 374 29. L. Liang, Z. X. Hu, Y. Y. Huang, S. L. Duan, J. He, Y. Huang, Y. X. Zhao and X. L.
9
10 375 Lu, *J. Nanosci. Nanotechnol.*, 2016, **16**(12), 12099-12111.
11
12 376 30. T. D. Meyer, S. Muyldermans and A. Depicker, *Trends in Biotechnology.*, 2014,
13
14 377 **32**(5), 263-270.
15
16 378 31. P. Sroga, D. Safronetz and D. R. Stein, *Future Virol.*, 2020, **15**(3), 195-205.
17
18 379 32. Q. Chen, Y. Y. Wang, F. J. Mao, B. C. Su, K. L. Bao, Z. L. Zhang, G. F. Xie and X.
19
20 380 Liu, *RSC Adv.*, 2020, **10**(56), 33700-33705.
21
22 381 33. Z. C. Sun, Z. H. Duan, X. Liu, X. Deng and Z. W. Tang, *Food Anal. Methods.*,
23
24 382 2017, **10**, 3558-3564.
25
26 383 34. G. Frens, *Nature (London), Phys. Sci.*, 1973, **241**(105), 20-22.
27
28 384 35. S. Thobhani, S. Attree, R. Boyd, N. Kumarswami, J. Noble, M. Szymanski and R.
29
30 385 A. Porter, *J. Immunol. Methods.*, 2010, **356**(1-2), 60-69.
31
32 386 36. C. Zhang, Y. Zhang and S. Wang, *J. Agric. Food Chem.*, 2006, **54**(7), 2502–2507.
33
34
35
36
37
38
39
40
41
42
43
44
45
46
47
48
49
50
51
52
53
54
55
56
57
58
59
60



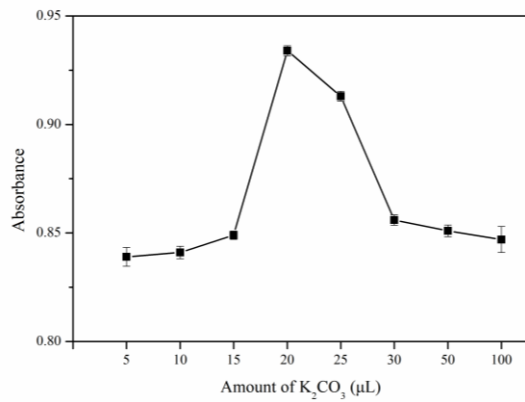
387

388

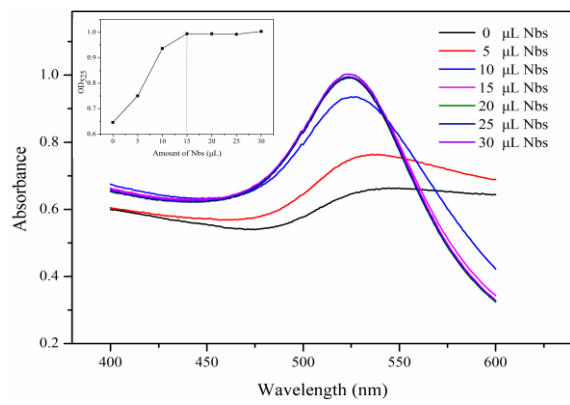
389 **Figure 1.** Nbs-based flow-through dot ELISA. (a) Optimization of Nbs and HRP-conjugated
390 6*his-tag McAb; (b) a series of concentrations of 3-PBA detected by Nbs-based flow-through dot
391 ELISA.

392

393



(a)



(b)

394

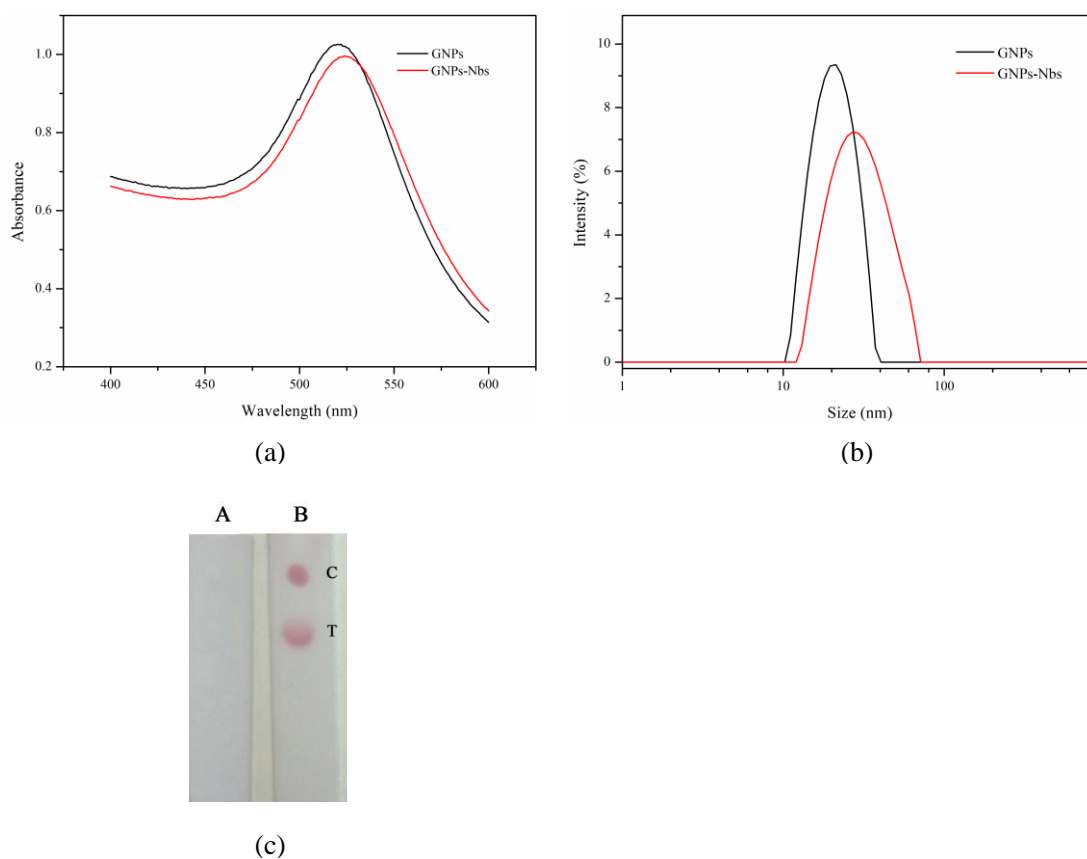
395

396 **Figure 2.** Optimization of GNPs labeling Nbs. (a) amount of K_2CO_3 (n=3); (b) amount of Nbs.

397

398

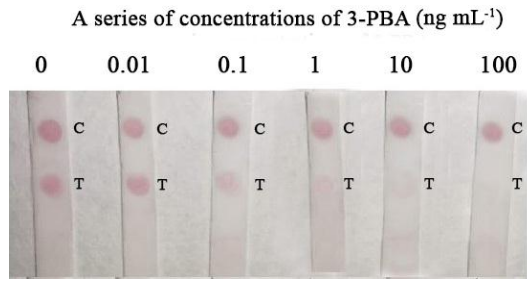
399



400

401 **Figure 3.** Verification of GNPs-Nbs. (a) scanning spectra of GNPs and GNPs-Nbs; (b) particle
402 size analysis of GNPs and GNPs-Nbs; (c) verification of GNPs-Nbs by lateral-flow immunoassay:
403 GNPs (A); GNPs-Nbs (B).

404

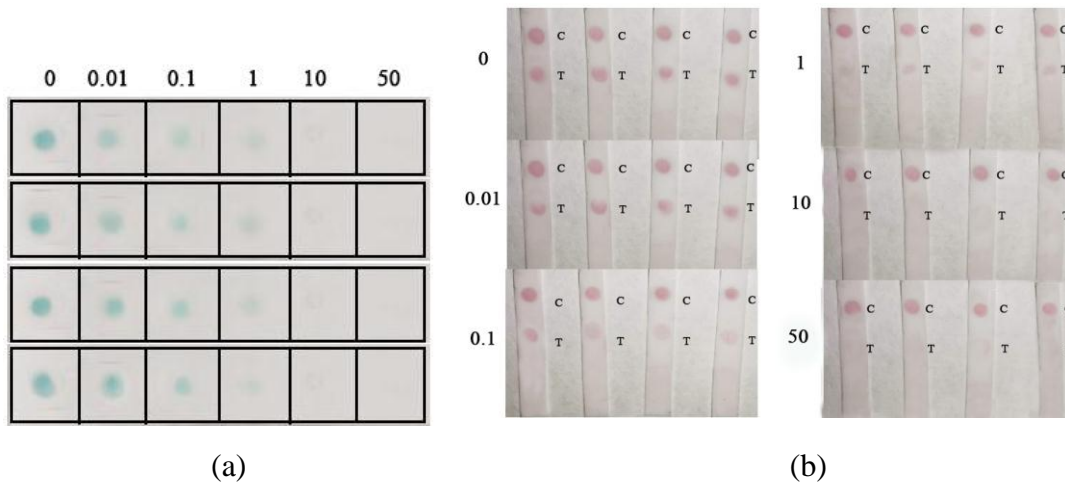


406 **Figure 4.** A series of concentrations of 3-PBA detected by GNPs-Nbs lateral-flow immunoassay.

407

1
2
3
4
5
6
7
8
9
10
11
12
13
14
15
16
17
18
19
20
21
22
23
24
25
26
27
28
29
30
31
32
33
34
35
36
37
38
39
40
41
42
43
44
45
46
47
48
49
50
51
52
53
54
55
56
57
58
59
60

408

3-PBA spiked in negative urine samples (ng mL^{-1})

409

410

411 **Figure 5.** Spiked samples analysis (n=4). (a) Nbs-based flow-through dot ELISA; (b) GNPs-Nbs
412 lateral-flow immunoassay.

413

414 **Table 1.** Cross-reactivity detected by Nbs-based flow-through dot ELISA, GNPs-Nbs lateral-flow
 415 immunoassay and plate ELISA.

Analytes	Chemical Structures	Cross-reactivity		
		Flow-through dot ELISA	Lateral-flow Immunoassay	Plate ELISA
3-phenoxybenzoic acid				100%
3-phenoxybenzaldehyde				75.1%
4-(3-hydroxybenoxy)benzoic acid				13.5%
3-phenoxybenzyl alcohol				<0.1%

416

417

418 **Table 2.** Spiked negative samples detected by Nbs-based flow-through dot ELISA, GNPs-Nbs
 419 lateral-flow immunoassay and LC-MS (n = 4).

3-PBA Spiked (ng mL ⁻¹)	Visual results ^a		LC-MS ^b (ng mL ⁻¹)	LC-MS Recovery (%)
	Flow-through Dot ELISA	Lateral-flow Immunoassay		
0.1	+, +, +, +	-/+, +, -/+, +	0.097 ± 0.070	97
1	+, +, +, +	+, +, +, +	0.981 ± 0.045	98
10	+, +, +, +	+, +, +, +	10.3 ± 0.8	103
50	+, +, +, +	+, +, +, +	50.7 ± 2.6	101

420 +: positive, the dot color is weak than control; -: negative, the dot color is bright than control; -/+:

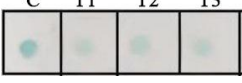
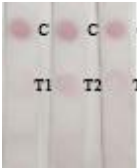
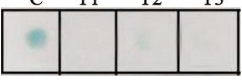
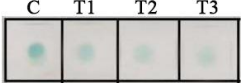
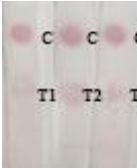
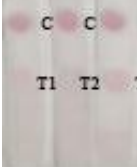
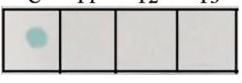
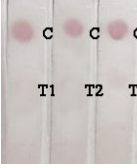
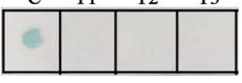
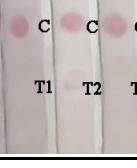
421 negative/positive, the dot color is around control

422 a. qualitative detection by Nbs-based flow-through dot ELISA, GNPs-Nbs lateral-flow
 423 immunoassay

424 b. quantitative analysis by LC-MS

425

426 **Table 3.** Randomly spiked samples analyzed by Nbs-based flow-through dot ELISA, GNPs-Nbs
 427 lateral-flow immunoassay and LC-MS.

Sample	Visual results (n = 3)			LC-MS (ng mL ⁻¹)	RSD (%)
	Flow-through dot ELISA	Lateral-flow Immunoassay			
U1				45.1 ± 1.1	2.4
U2				1.11 ± 0.07	6.3
U3				22.6 ± 0.5	2.2
U4				0.67 ± 0.04	5.9
L1				4.63 ± 0.26	5.6
L2				11.7 ± 0.8	6.8
L3				2.47 ± 0.12	4.8
L4				50.7 ± 1.6	3.2

428 U and L: randomly spiked in urine (U) and lake water (L) samples, respectively;

429 C: control; T1-T3: repeated sample detection